Published in final edited form as:
Pediatr Cardiol. 2014 October ; 35(7): 1295–1300. doi:10.1007/s00246-014-0946-y.

Investigational Lymphatic Imaging at the Bedside in a Pediatric Postoperative Chylothorax Patient

I-Chih Tan,
Center for Molecular Imaging, Institute of Molecular Medicine, The University of Texas Health Science Center, Houston, TX 77030, USA

John C. Rasmussen,
Center for Molecular Imaging, Institute of Molecular Medicine, The University of Texas Health Science Center, Houston, TX 77030, USA

Eva M. Sevick-Muraca,
Center for Molecular Imaging, Institute of Molecular Medicine, The University of Texas Health Science Center, Houston, TX 77030, USA

Duraisamy Balaguru,
Division of Pediatric Cardiology, The University of Texas Health Science Center, Houston, TX 77030, USA

John T. Bricker,
Division of Pediatric Cardiology, The University of Texas Health Science Center, Houston, TX 77030, USA

Renie Guilliod, and
Division of Cardiology and Hyperbaric Medicine, The University of Texas Health Science Center, Houston, TX 77030, USA

William I. Douglas
Division of Pediatric Cardiovascular Surgery, The University of Texas Health Science Center, Houston, TX 77030, USA

Abstract

Background—Chylothorax is a rare but serious complication in children who undergo heart surgery. Its pathogenesis is poorly understood, and invasive surgical treatments are considered only after conservative management fails. Current diagnostic imaging techniques, which could aid decision making for earlier surgical intervention, are difficult to apply. Herein, we deployed near-infrared fluorescence (NIRF) lymphatic imaging to allow the visualization of abnormal lymphatic drainage in an infant with postoperative chylothorax to guide the choice of surgical management.

i-chih.tan@uth.tmc.edu.

Conflict-of-interest statement. E. M. Sevick-Muraca declares financial interest in the NIRF Imaging, Inc., a company seeking to commercialize NIRF lymphatic imaging. I-C Tan, J. C. Rasmussen, and E. M. Sevick-Muraca also are inventors on patents and patent applications concerning the technology presented herein.

Methods—A 5-week-old male infant, who developed chylothoraces after undergoing Norwood surgery for hypoplastic left heart syndrome, was intradermally administered trace doses of indocyanine green in both feet and the left hand. NIRF imaging was then performed at the bedside to visualize lymphatic drainage patterns.

Results—Imaging results indicated impeded lymphatic drainage from the feet toward the trunk with no fluorescence in the chest indicating no leakage of peripheral lymph at the thoracic duct. Instead, lymph drainage occurred from the axilla directly into the pleural cavity. As a result of imaging, left pleurodesis was performed to stop the pleural effusion with the result of temporary decrease of left chest tube drainage.

Conclusion—Although additional studies are required to understand normal and abnormal lymphatic drainage patterns in infants, we showed the potential of using NIRF lymphatic imaging at the bedside to visualize the lymphatic drainage pathway to guide therapy. Timely management of chylothorax may be improved by using NIRF imaging to understand lymphatic drainage pathways.

Keywords

Near-infrared fluorescence imaging; Chylothorax; Congenital heart defect; Postoperative care

Introduction

Chylothorax is serious complication in children who undergo heart surgery and is associated with high morbidity and mortality rates [1, 2]. The incidence of chylothorax after cardiac surgery in children is estimated to be 1.3 % to 9.2 %, and this has increased significantly in the last two decades [1, 3–7]. Pathogenesis of chylothorax is poorly understood but is thought to arise from (1) direct damage to the thoracic duct by rupture, laceration, tear, or compression, (2) central venous (CV) obstruction, or (3) high CV pressure that impedes thoracic duct drainage into the venous system.

Initial conservative management for chylothorax consists of gut rest as well as dietary modification and sometimes administration of octreotide to decrease the chyle production. Surgical treatments, such as pleurodesis and thoracic duct ligation, are considered as a last resort if conservative management fails. Thoracic duct ligation or pleurodesis have only limited success in treating chylothorax [5]. Improving the poor response to these therapies demands a better understanding of the specific lymphatic drainage mechanisms responsible for the onset of chylothorax. The inability to image lymphatics of infants cared for within pediatric intensive care units (PICU) has limited the understanding of the pathogenesis of chylothorax, which in turn has impeded the application of appropriate and timely management for these critically ill children. Recently, the near-infrared fluorescence (NIRF) imaging technique has been successfully used in adults to assess the lymphatic vasculature and its function [8–11] as well as response to therapy [12,13] and in infants with lymphatic dysfunction [14]. After an intradermal injection of indocyanine green (ICG), the dye is rapidly taken up by the lymphatic vasculature. The fluorescence emanating from the ICG enables the visualization of the lymphatic architecture and contractile function (for review see [15]).Herein, we present a Food and Drug Administration (FDA) emergency–use case of

bedside application of NIRF lymphatic imaging in PICU to guide surgical therapy in an infant with bilateral chylothoraces after surgery for hypoplastic left heart syndrome (HLHS).

Materials and Methods

The protocol used for this study was approved by the FDA (IND 115,796) and the Institutional Review Board at the University of Texas Health Science Center for the off-label use of ICG.

Patient and Interventions

NIRF imaging was sought to guide surgical management of chylothorax in a 5-week-old male infant weighing 3.1 kg. The infant was born with HLHS, and at 5 days of age he underwent Norwood surgery. After surgery, the baby developed bilateral chylothoraces and chyloascites. Initially, fluid drainage per day totaled approximately 300 ml.

Conservative management of medium chain triglyceride–based infant formula feed was instituted followed by a trial of total parenteral nutrition without any enteral feeding. These management strategies failed and daily drainage remained at approximately 185 ml. On postoperative day 14, octreotide infusion was started. On postoperative day 18, octreotide treatment was deemed ineffective and stopped. Doppler study of the subclavian veins showed patency of subclavian and jugular veins on both sides. Multiple echocardiograms confirmed normal ventricular systolic function. No atrioventricular or neoaortic valve regurgitation or coarctation in the aortic arch was present. Cardiac catheterization to measure left-ventricular end-diastolic pressure was not performed. Surgical treatments for chylothorax were considered, and NIRF lymphatic imaging was sought to help decide whether pleurodesis or thoracic duct ligation would be more appropriate. After parental informed consent was obtained, investigational NIRF lymphatic imaging was performed at the bedside in the PICU without any alteration or interruption to the existing care of the baby.

NIRF Lymphatic Imaging

The instrumentation and imaging method employed were previously described by Rasmussen *et al*. [16]. The baby's eyes were covered with black vinyl tape on top of a gauze pad to prevent the unlikely damage by the dim excitation laser light (<1.9 mW/cm^2). Twenty-five mcg of ICG in 0.1 cc of saline was first injected intradermally into the dorsum of left foot with expectation to visualize its transport through the lymphatics of the leg to the thoracic duct as shown in Figure 1A. The baby was kept in a supine position under the camera during the initial part of imaging as shown in Figure 1B. NIRF images were obtained from the leg, groin, and trunk area. A second injection of 12.5 mcg of ICG in 0.05 cc of saline was administered to the dorsum of right foot 19 minutes after the first injection. A third injection of 12.5 mcg of ICG in 0.05 cc of saline was administered to the dorsum of left hand 26 minutes after the second injection, and imaging was continued for another 90 minutes. During that time, the baby was briefly placed into right lateral recumbent position to allow imaging of his back. Recorded NIRF image sequences were later analyzed to observe the dynamic transit of lymphatic drainage from the extremities toward the trunk.

There were no adverse events associated with the imaging and no apparent reactions to the ICG.

Results

NIRF images allowed visualization of the lymphatic drainage proximally from the ICG injection sites in both feet and the left hand. Figure 2 shows the schematic of the body with the field of view marked (Fig. 2A) as well as the NIRF image acquired 16 minutes after the second injection (Fig. 2B). Lymph transiting from both feet toward the groin was seen, but no fluorescence was observed above the groin. Extralymphatic leakage of ICG was seen in both legs. At this stage, images acquired from the chest or clavicular regions showed no fluorescence suggesting that there was no ICG drainage toward chest through the thoracic duct 40 minutes after the injections in the feet.

Figure 3 shows sequential NIRF images acquired after the injection made in the left hand and the corresponding schematic. The patches on the chest are outlined in the NIRF images to provide anatomical reference. The ICG drained from the hand toward the axilla as seen in Figures 3B to 3D. However, after reaching the axilla, the ICG drainage did not continue toward the infraclavicular area and drain into the venous system as expected. Instead, the ICG drained retrograde into the left side of chest as seen in Figures 3E to 3F. ICG fluorescence appeared to first outline the pleural cavity, bordered below by diaphragm, and stop approximately at the midline as seen in Figures 3G to 3I. Figure 4 shows later images where the fluorescence crossed the midline to the right side of the chest as seen in Figure 4(a), and eventually filled the whole right chest as seen in Figure 4B.

To confirm whether the fluorescence outlined the pleural cavity, the baby was turned to the right side as shown in Figure 4C, and a dorsal view NIRF image of the trunk was acquired 54 minutes after ICG injection in the left hand. Fluorescence was noted in whole of the left hemithorax that may correspond to left pleural cavity.

These findings were interpreted as follows: ICG injections in both feet drained only up to the groin level due to high CV pressure. Drainage from the left-hand injection stopped at the axilla also due to high CV pressure. Lymph from left arm drained in a retrograde direction toward lower resistance and accumulated in the left pleural cavity.

Per the results of imaging, we decided that the best option was to perform bilateral pleurodesis, one side at a time, to block the low resistance pathways for lymphatic drainage. Left pleurodesis was performed first, and left chest tube drainage decreased. However, coincident to the decrease in left chest tube drainage, abdominal distension from chylous ascites appeared. Right pleurodesis was not performed due to the deterioration of the subject's clinical condition. Decision was made to offer “comfort care” as well as nonescalation of care. The subject died, and no postmortem examination was performed.

Discussion

Our interpretation of NIRF images was based on previous experience in cases of adults and older children with lymphedema from different causes in different parts of the body. We did

not have an opportunity to demonstrate leakage in the thoracic duct, probably due to high CV pressure, or obstruction to lymphatics preventing ICG transport from the groin toward the chest. Images after the left-hand injection are interesting and raised three points that affected surgical management: (1) lymphatic flow from the left arm was impeded beyond axilla due to a significant increase in CV pressure; (2) alternative pathway to drain was found; and (3) this contributed at least in part to fluid accumulated in the pleural space. The observations of drainage from the left axilla into the pleural space could explain why decreasing mesenteric lymph production with dietary treatment had failed to resolve the condition.

Since our study performed in June 2012, Shibaski *et al.* have published similar lymphatic imaging results on infants and neonates with congenital pleural effusion and ascities using subcutaneous injections of 250 mcg of ICG in the web space of the hands and feet to show that lymphatic mapping was consistent with clinical assessment of mild, moderate, or severe lymphatic dysplasia [14]. To our knowledge, our study is the first case reported using NIRF imaging in an infant to guide therapy.

Instances of lack of response to surgical ligation of the thoracic duct raise the question of whether thoracic duct injury is the cause of the pleural effusion. One of the challenges for predicting outcomes arises from the potential anatomical variation in course and drainage of the thoracic duct in individuals [17]. Visualization of the thoracic duct and the accessory lymphatics, as well as identification of leak sites (if any), would show the possible etiology of the chylothorax and allow optimal treatment strategy.

There were limitations to this study. First, although NIRF imaging can detect ICG as deep as 3 to 4 cm in the tissues [18], there was no definitive proof that ICG fluorescence from the thoracic duct could be detected in an infant. Although no fluorescence was detected from the chest area after the first two injections, we could not definitely rule out the possibility of ICG presence in the thoracic duct. In addition, the 45 minutes that elapsed between the initial injections in the feet and the injection in left hand may not have been sufficient to enable ICG transport, although the transit times from the foot to the leg in adults occurs in a matter of a few minutes. [16] Both potential limitations could have prevented the identification of leakage site at the thoracic duct using NIRF imaging. However, Shibasaki *et al*. performed imaging at 3 to 6 and 24 hours after ICG administration and showed superficial lymphatic channels in the abdomen [14]. Due to the need for intervention, we did not conduct imaging >2.5 hours after ICG administration, and lymphatic channels outside of the arm and legs were not seen. Second, no injection was made in the right hand preventing visualization of the lymphatic drainage pattern on the right side of the upper body, which could have also contributed to the chylothorax. Third, due to the deteriorating condition of the infant, no imaging was performed after pleurodesis. The effect on the lymphatic drainage pattern that could have been used to assess the outcome of the surgical treatment was unknown.

In conclusion, we present a case of NIRF lymphatic imaging to guide the choice of surgical intervention in an infant who developed chylothorax after congenital heart surgery. The ability to perform imaging at the bedside in an intensive care unit setting is an important

development. The mechanism of pleural effusion other than thoracic duct leakage can be explored using such noninvasive imaging. Continued experience with lymphatic imaging will help advance the understanding of the pathogenesis of chylothorax or prolonged pleural effusion and could improve the treatment strategies.

Acknowledgments

This study was supported in parts by National Institutes of Health Grants No. R01 HL092923 and U54 CA136404.

References

1. Zuluaga MT. Chylothorax after surgery for congenital heart disease. Curr Opin Pediatr. 2012; 24(3): 291–294. [PubMed: 22498675]
2. Soto-Martinez M, Massie J. Chylothorax: Diagnosis and management in children. Paediatr Respir Rev. 2009; 10(4):199–207. [PubMed: 19879510]
3. Milonakis M, Chatzis AC, Giannopoulos NM, Contrafouris C, Bobos D, Kirvassilis GV, et al. Etiology and Management of chylothorax following pediatric heart surgery. J Card Surg. 2009; 24(4):369–373. [PubMed: 19583606]
4. Pego-Fernandes PM, Nascimbem MB, Ranzani OT, Shimoda MS, Monteiro R, Jatene FB. Video-assisted thoracoscopy as an option in the surgical treatment of chylothorax after cardiac surgery in children. J Brasil Pneumol. 2011; 37(1):28–35.
5. Chan EH, Russell JL, Williams WG, Van Arsdell GS, Coles JG, McCrindle BW. Postoperative chylothorax after cardiothoracic surgery in children. Ann Thorac Surg. 2005; 80(5):1864–1870. [PubMed: 16242470]
6. Biewer E, Zürn C, Arnold R, Glöckler M, Schulte-Mönting J, Schlensak C, et al. Chylothorax after surgery on congenital heart disease in newborns and infants—Risk factors and efficacy of MCT-diet. J Cardiothorac Surg. 2010; 5(1):1–7. [PubMed: 20064238]
7. Matsuo S, Takahashi G, Konishi A, Sai S. Management of refractory chylothorax after pediatric cardiovascular surgery. Pediatr Cardiol. 2013; 34(5):1094–1099. [PubMed: 23229292]
8. Rasmussen JC, Tan IC, Marshall MV, Fife CE, Sevick-Muraca EM. Lymphatic imaging in humans with near-infrared fluorescence. Curr Opin Biotechnol. 2009; 20(1):74–82. [PubMed: 19233639]
9. Okitsu T, Tsuji T, Fujii T, Mihara M, Hara H, Kisu I, et al. Natural history of lymph pumping pressure after pelvic lymphadenectomy. Lymphology. 2012; 45(4):165–176. [PubMed: 23700763]
10. Mihara M, Seki Y, Hara H, Iida T, Oka A, Kikuchi K, et al. Predictive lymphatic mapping: A method for mapping lymphatic channels in patients with advanced unilateral lymphedema using indocyanine green lymphography. Ann Plast Surg. 2013; 72(6):706–710. [PubMed: 23486121]
11. Burrows PE, Gonzalez-Garay ML, Rasmussen JC, Aldrich MB, Guilliod R, Maus EA, et al. Lymphatic abnormalities are associated with RASA1 gene mutations in mouse and man. Proc Natl Acad Sci U S A. 2013; 110(21):8621–8626. [PubMed: 23650393]
12. Adams KE, Rasmussen JC, Darne C, Tan I-C, Aldrich MB, Marshall MV, et al. Direct evidence of lymphatic function improvement after advanced pneumatic compression device treatment of lymphedema. Biomed Opt Express. 2010; 1(1):114–125. [PubMed: 21258451]
13. Tan IC, Maus EA, Rasmussen JC, Marshall MV, Adams KE, Fife CE, et al. Assessment of lymphatic contractile function after manual lymphatic drainage using near-infrared fluorescence imaging. Arch Phys Med Rehabil. 2011; 92(5):756–764. e751. [PubMed: 21530723]
14. Shibasaki J, Hara H, Mihara M, Adachi S, Uchida Y, Itani Y. Evaluation of lymphatic dysplasia in patients with congenital pleural effusion and ascites using indocyanine green lymphography. J Pediatr. 2014; 164(5):1116–1120.e1. [PubMed: 24518167]
15. Sevick-Muraca EM, Kwon S, Rasmussen JC. Emerging lymphatic imaging technologies for mouse and man. J Clin Invest. 2014; 124(3):905–914. [PubMed: 24590275]
16. Rasmussen JC, Tan IC, Marshall MV, Adams KE, Kwon S, Fife CE, et al. Human lymphatic architecture and dynamic transport imaged using near-infrared fluorescence. Transl Oncol. 2010; 3(6):362–372. [PubMed: 21151475]

17. Hematti H, Mehran RJ. Anatomy of the thoracic duct. Thorac Surg Clin. 2011; 21(2):229–238. [PubMed: 21477773]

18. Sevick-Muraca EM, Sharma R, Rasmussen JC, Marshall MV, Wendt JA, Pham HQ, et al. Imaging of lymph flow in breast cancer patients after microdose administration of a near-infrared fluorophore: Feasibility study. Radiology. 2008; 246(3):734–741. [PubMed: 18223125]

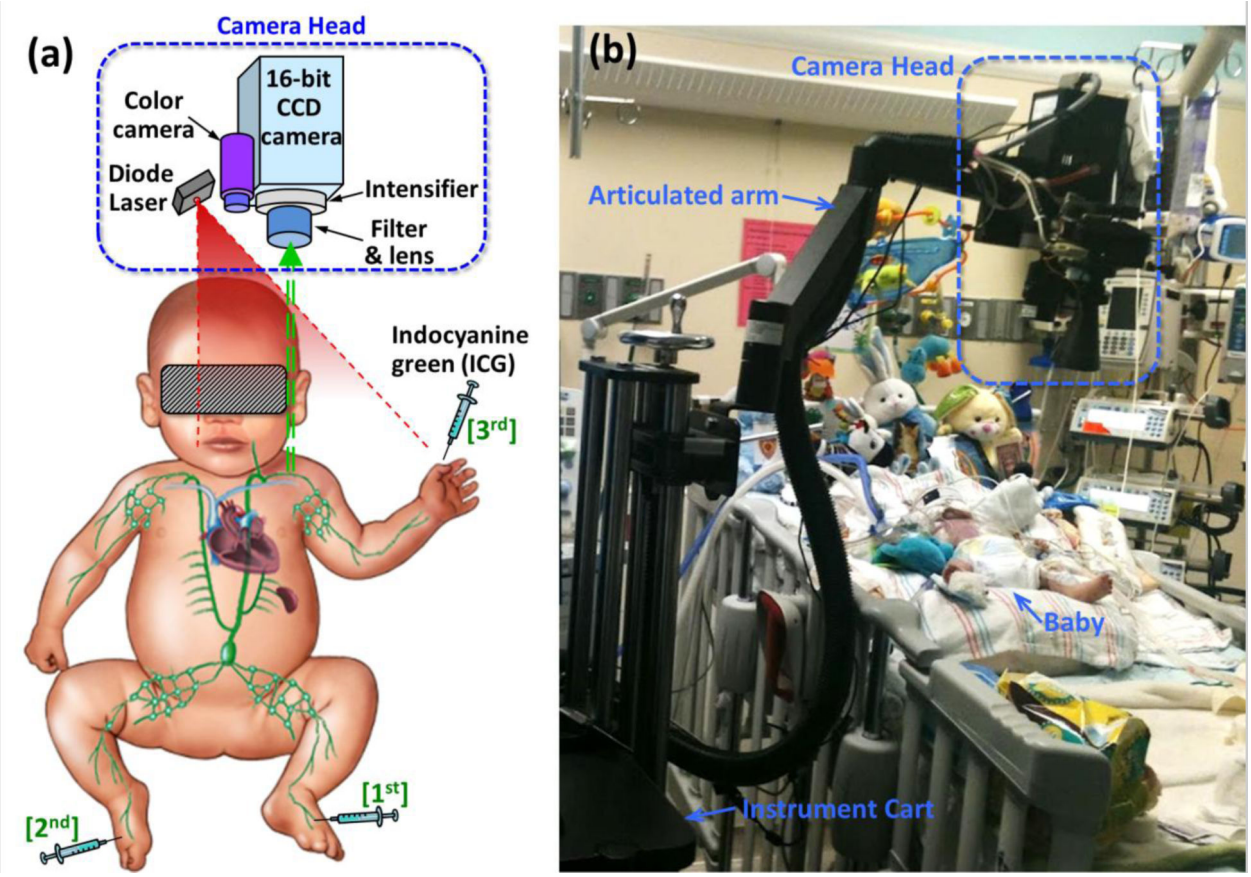

Fig. 1.

(**A**) Illustration of NIRF imaging principle and instrumentation. (**B**) Photo of the setup for NIRF imaging at the bedside in the PICU.

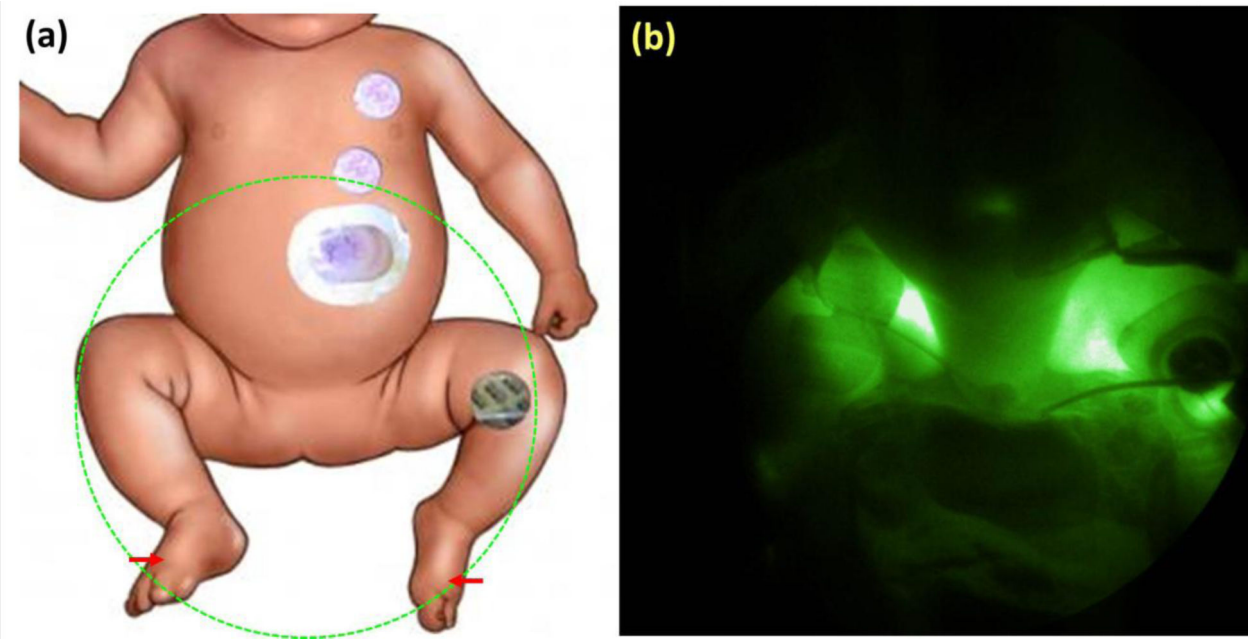

Fig. 2.

(**A**) Schematic of corresponding field of view with injection site marked by arrows. (**B**) NIRF image of groin area >16 minutes after intradermal injections of ICG in both feet.

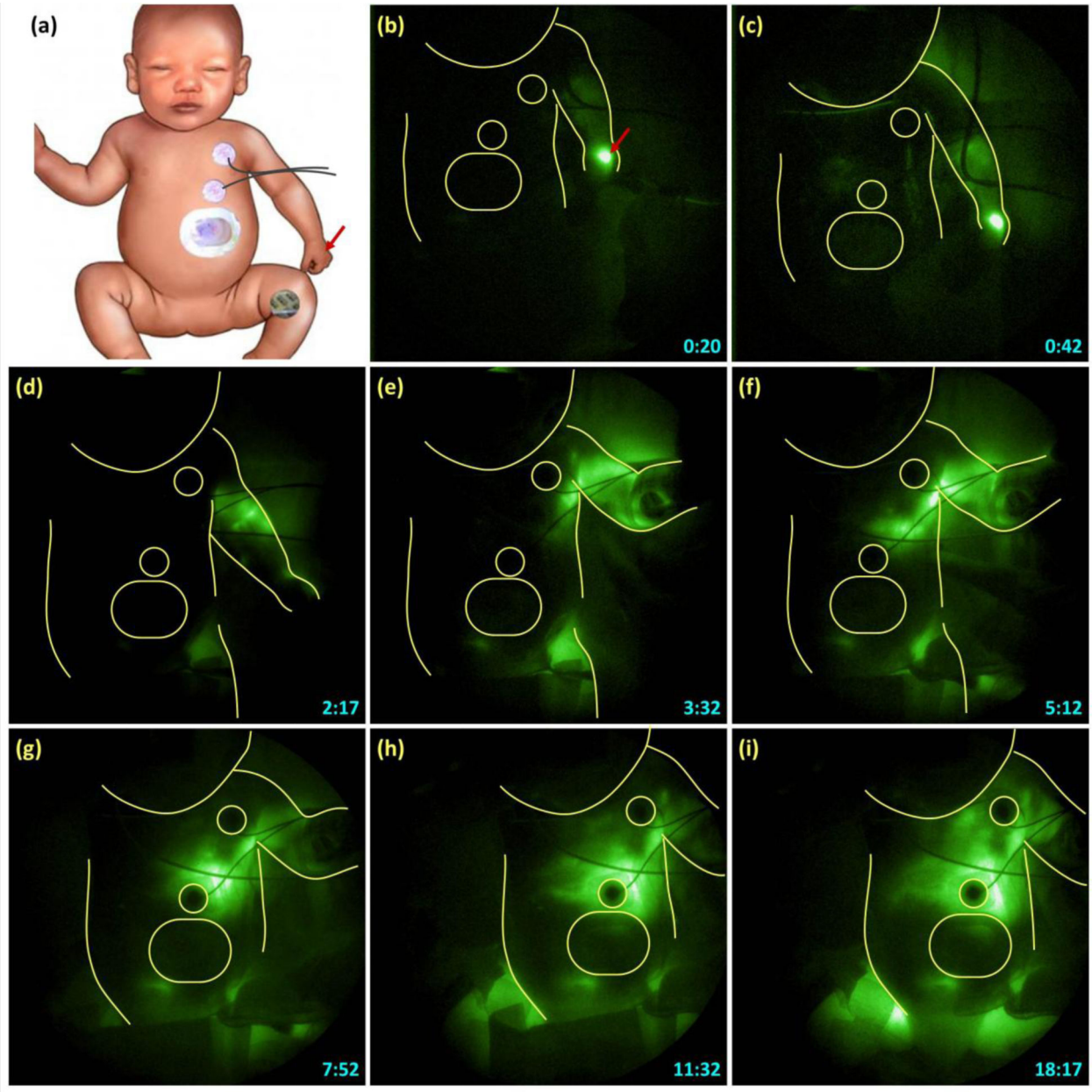

Fig. 3.

Time-lapse images (**B through I**) of NIRF lymphatic images after intradermal injection of ICG in the left hand, the site of which is marked by the arrow in schematic (Fig. 3A). Time-stamp in the right lower corner indicates time in minutes and seconds after the injection. The patches on the chest are outlined to provide anatomical reference.

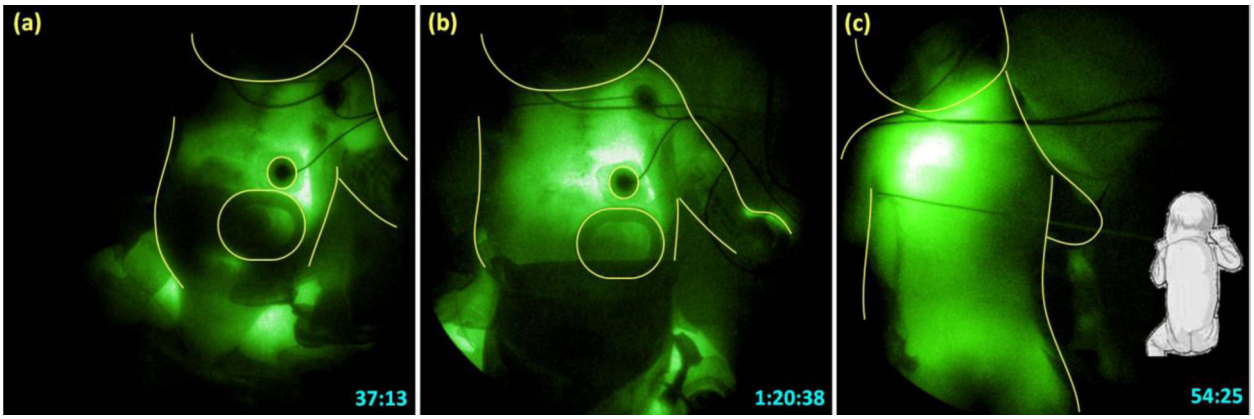

Fig. 4.

NIRF image of the trunk in ventral view at (**A**) 37 and (**b**) 80 minutes and (**C**) in dorsal view at 54 minutes after ICG injection in the left hand.